



# Radio Astronomy

## Lecture 3

### Science of Radio Astronomy: Galactic and Solar System

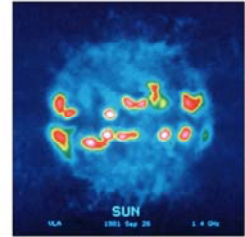
Lecturer: Joeri van Leeuwen ([leeuwen@astron.nl](mailto:leeuwen@astron.nl))

April 10<sup>th</sup> 2017



# Outline

- Solar system: Sun, planets
- Galactic: gas, (proto-)stars, compact objects, exoplanets, seti



- Today I talk about emission from Galactic and Solar System objects.
- At visible wavelengths all the emission seen from the Galactic objects is due to light reflected from the sun. However at radio wavelengths there is very little reflected sunlight so the radio emission observed from many planets is dominated by thermal emission. This emission is related to the surface temperature of these bodies.

# Solar System

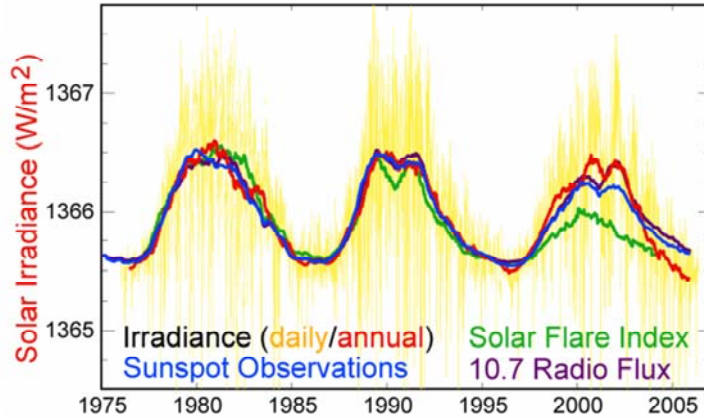
- Radio emission can be observed from many bodies in the solar system
- Both the active and quiet sun emit radio waves
- Planets can be observed as thermal sources (black body radiation)
- Magnetic planets have radio emitting radiation belts
- Comets emit 18 cm OH line radiation

- Other emission, as we will see, is non-thermal;
- And some radio observations in the Solar System are “active”, i.e., based on radar.

# Sun

Radio emission from sun correlates well with solar activity

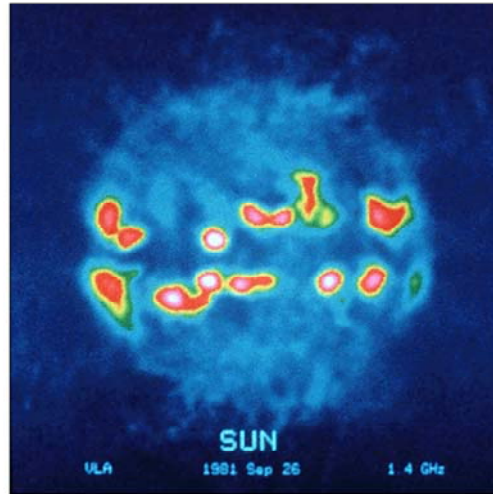
## Solar Cycle Variations



- The quiet sun component of the radio emission is from thermal emission from the hot ionized gas. The main source of opacity in the sun's atmosphere (the photosphere, chromosphere and corona) at radio wavelengths comes from electrons. The bulk of the emission arises from the region where the opacity is near 1. At visible wavelengths this happens at the photosphere where the temperature is about 6000 K and hence the sun appears as a blackbody with that temperature. At a frequency of 100 GHz (wavelength 0.3cm) the emission originates at the same height in the photosphere and the sun appears as a 6000 K blackbody. But at a frequency of 1.4 GHz (wavelength of 21 cm) the emission originated from the top of the chromosphere and is seen as a blackbody of temperature of about 100,000 K. And at longer wavelengths (300 cm or frequency of 0.1 GHz) the emission arises from the corona and is a 2 million K blackbody. This also means that the size of the sun measured at the different wavelengths will vary.

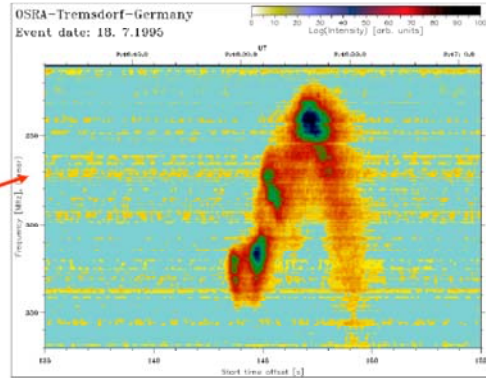
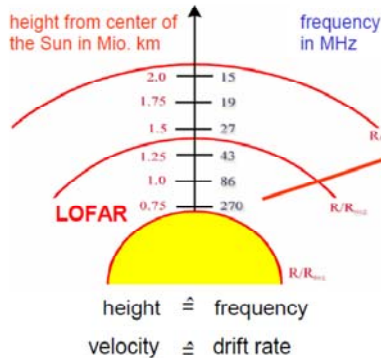
# Sun

Radio image of sun showing disk and active regions



- The other two components are related to the sunspot activity on the sun. The slowly varying component is also thermal in origin and arises from the region above the sunspots where the electron density is higher. The blackbody temperature of these regions can be as high as 2 million K. Thus the regions above the sunspots can contribute more radio emission than the total area without sunspots and increase the total radio flux relative to the quiet sun. So the change in the total radio flux is dependent on the total number of sunspots. The radio flux density then follows the 11 year sunspot cycle.

# Sun



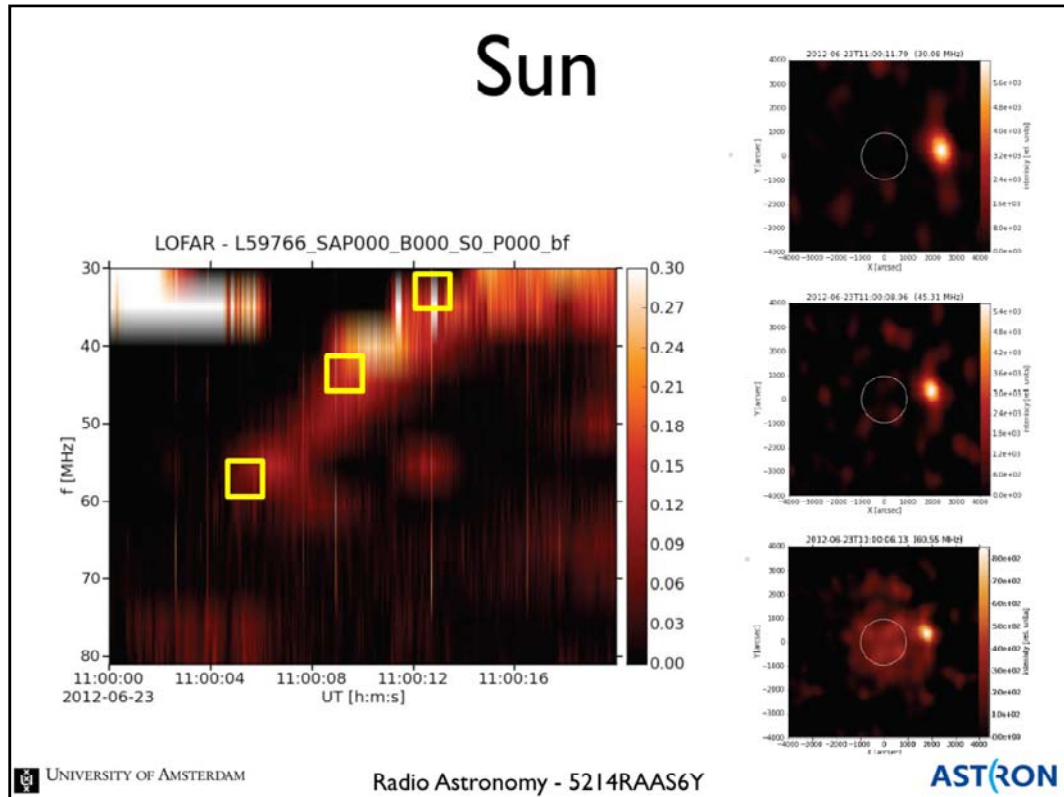
dynamic radio spectrogram ↔ height-time diagram

$$f_{pe} = \frac{1}{2\pi} \sqrt{\frac{e^2 N_e}{\epsilon_0 m_e}}$$

plasma frequency

- Solar flares are certainly among the most dramatic and energetic fast processes in our solar system that we know of.
- Major fractions of the flare-accelerated electrons and protons escape into space, in a “Solar Type III burst”.
- Electrons accelerated in solar flares to energies of some keV are streaming away from the Sun and excite plasma oscillations locally, all the way from the corona into the distant heliosphere, the frequency  $f_{pe}$  being determined by the local electron density  $N_e$ . These plasma oscillations (sometimes also called Langmuir waves) are converted to escaping electromagnetic radiation (of the same frequency or its harmonic) by non-linear wave-wave interactions.
- Because of the outward travel of the electrons (left) through the radial density gradient the wave frequency gradually decreases with time, and their onset times are gradually delayed. That leads to the characteristic frequency variation of type III bursts as shown on the right (watch out for the inverted frequency scale!)

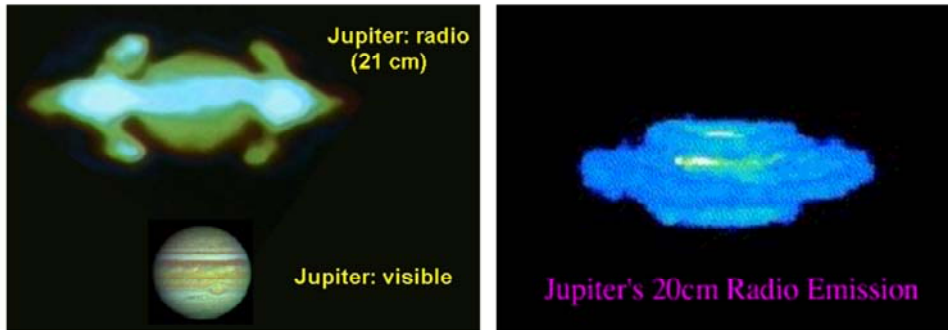
# Sun



- LOFAR has the unique capability of making simultaneous dynamic spectra (left) and images (right).
- In this early plot, you can see the burst move out (from bottom to top in right-most column)

# Giant Planets

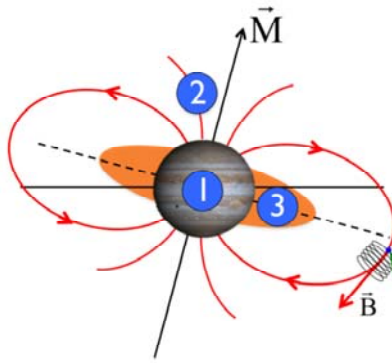
## Radio emission from Jupiter's radiation belts



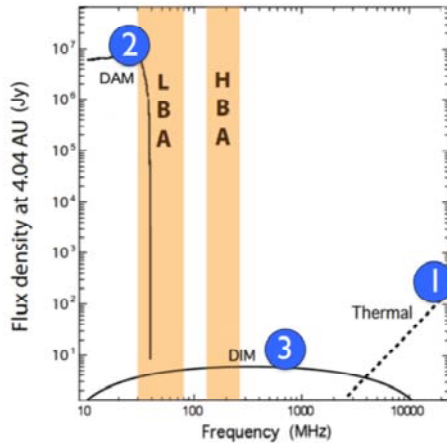
- The Jovian planets are cold. Jupiter, however, is a strong radio emitter at the long (> 10cm) radio wavelengths. At shorter wavelengths (around 3 cm) Jupiter has a brightness temperature of around 140 K which is consistent with infrared measurements (cf. [1] on next slide)



# Giant Planets

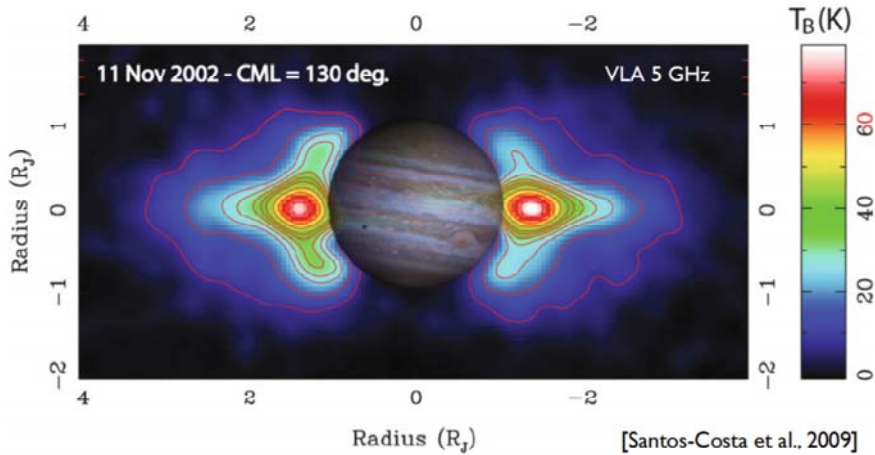


- 1 Thermal ( $\lambda \sim \text{cm}$ )
- 2 Auroral / Io cyclotron emission ( $\lambda \geq \text{Dm}$ )
- 3 Radiation belts synchrotron emission ( $\lambda = \text{cm-dm-m}$ )



- However at longer wavelengths the temperatures are of the order of a few thousand degrees. These high temperatures come from a nonthermal source namely synchrotron emission from the strong magnetic field of the planet [3], where DIM is Decimetric wavelength. Jupiter also has some strongly varying radio emission at longer radio wavelengths (DAM=Decametric). The source of this emission has been found to be nonthermal cyclotron emission [2]. This arises from electrons spiraling in Jupiter's magnetic field. The variation is caused by the fact that the origin of these electrons are the volcanoes and geysers on the surface of Io. Marked on the right are the Low Band Antenna and High Band Antenna ranges for LOFAR.

# Giant Planets

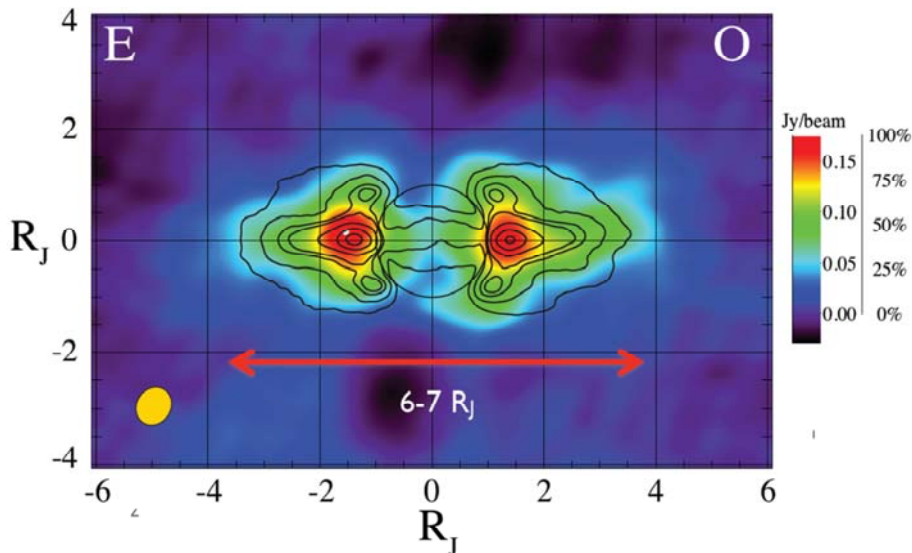


### 3 Radiation belts synchrotron emission ( $\lambda = \text{cm-dm-m}$ )

- Belts radiating from  $\sim 1$  to  $\sim 3 R_J$
- Energetic particles (ions, e- of 100s keV  $\rightarrow$  10s MeV) trapped near the magnetic equator
- Anisotropic (beamed) and polarized emission ( $\sim 20$ -25% linear,  $< 1\%$  circular)

# Giant Planets

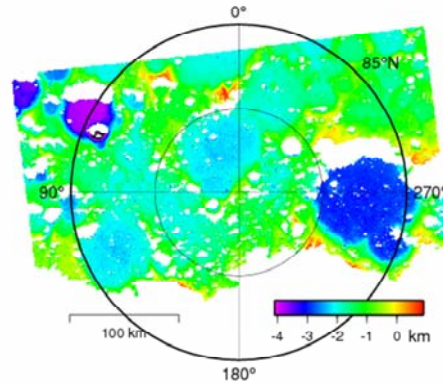
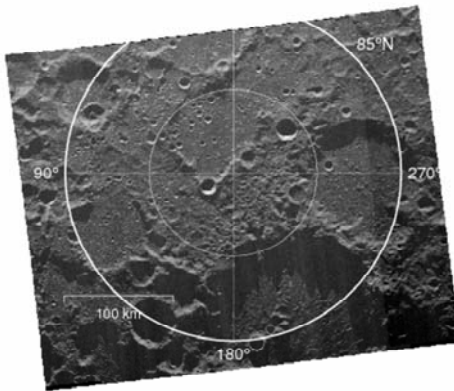
First LOFAR detections:



- Radio emission from the other Jovian planets has been found to be mainly thermal. The emission arises mainly from the cloud tops of the planet atmospheres and shows that the temperatures drop the farther the planet is from the sun.

# Moon

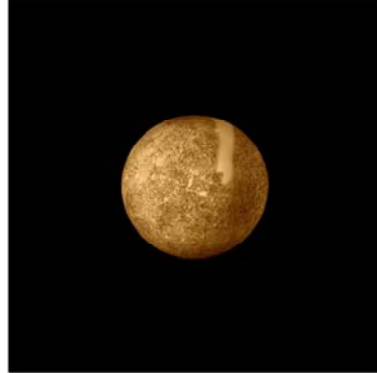
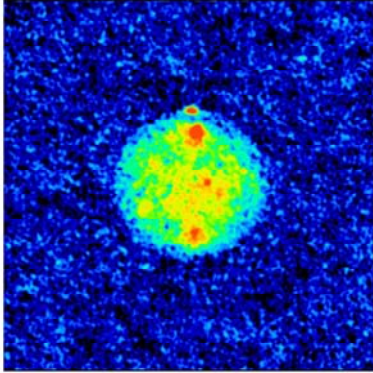
Modern lunar image near the north pole, and elevation in color



- Some emission from the moon is also thermal. At infrared wavelengths there are variations correlated to the lunar phase which are due to solar heating. At centimeter wavelengths this variation is much less. This is because the radio emission (which is still thermal) arises from below the surface.
- In active observing, lunar radar observing is done with Goldstone (75 meter resolution) and with Arecibo + Green Bank (20 meter resolution).

# Mercury

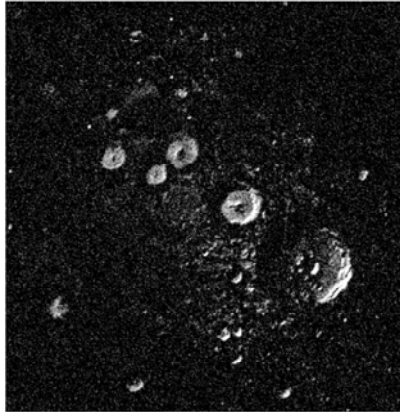
Radar image of Mercury - ice near north pole?



- This left image was made using the Jet Propulsion Lab (JPL) Goldstone transmitters, combined with the NRAO Very Large Array receivers, in a doppler radar experiment. Red areas show regions of the highest reflectivity; the northern red spot is due to water-ice resting in permanent shade on Mercury's pole. The origin of the other red areas are unknown.

# Mercury

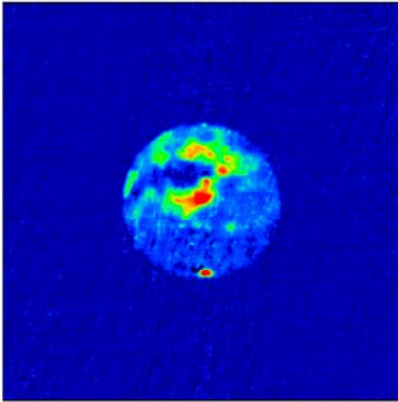
Arecibo delay-Doppler radar image, 450x450 km  
of Mercury's north pole, showing ice deposits



- One of the major recent successes in the field of planetary radar astronomy was the discovery and mapping of deposits of volatiles on the shadowed floors of impact craters at the poles of Mercury. Because of the similarity of their radar scattering properties to those of icy surfaces in the solar system, the deposits are thought to be water ice, permanently shadowed on crater floors. The figure shows the most recent Arecibo 12.6 cm (2.4 GHz, "S-band") radar image of the north polar region of Mercury made at a resolution of 1.5 km. The image measures 450 km on a side. The donut shape of the deposits close to the pole are due to the presence of central peaks in the craters while the bright arcs away from the poles coincide with the shadowed areas for these craters. A detection of the "ice" at the north pole was also obtained with the Arecibo 70 cm wavelength radar indicating that the deposits may be at least several meters thick.

# Mars

Radar image of Mars – again likely polar ice



- In this 1988 Goldstone-VLA radar image of Mars, like in the radar image of Mercury, the red areas represent surfaces of high reflectivity. The red regions in the center of the planet are associated with the giant volcanoes located there.

# Asteroids

The screenshot shows a CNN news article. At the top, the CNN logo is prominent, along with navigation links for various regions like U.S., Africa, Asia, Europe, Latin America, Middle East, Business, World Sport, Entertainment, Tech, Travel, and iReport. Below the navigation is a banner for 'the CNN Freedom Project' with the tagline 'Building a More Free World' and the URL 'CNN.com/freedom'. The main article headline is 'Forget falling stars: NASA plans to catch an asteroid' by Dana Ford, dated April 8, 2013. The article features a large image of an asteroid. To the right of the article is a 'SHARE THIS' section with social media icons for Facebook, Twitter, YouTube, and LinkedIn, along with options for Print, Email, and More sharing. Below the article is a 'Most Popular' section with a link to a story about North Korea's nuclear test. At the bottom right of the article area is a 'MAKE A WISH International' advertisement with the text 'A world of wishes awaits... Celebrate World Wish Day & help more wishes come true' and a 'JOIN THE WORLD' button.

- Radar imaging of near-Earth asteroids can provide dramatic images with resolutions down to 8 m, comparable to the images obtained by the Galileo and NEAR-Shoemaker spacecraft.



# Asteroids

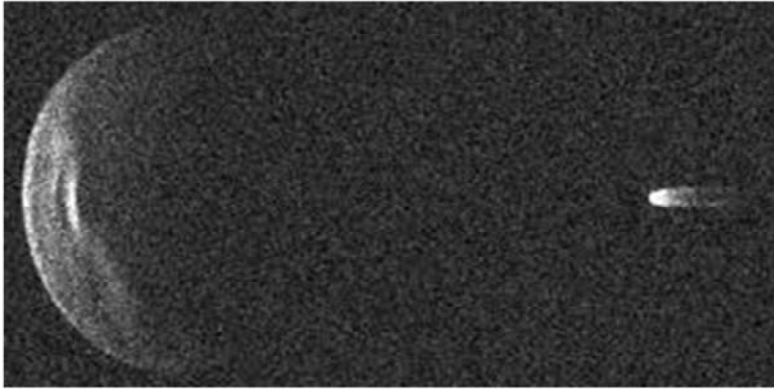
Arecibo delay-Doppler radar image of  
NEA 1999 JM8 (D ~ 7 km)



- Radar investigations of many Near Earth Asteroids (NEAs) are roughly equivalent, in their science content, to space flyby missions, but have a much lower cost (five orders of magnitude).
- The rotation rate, shape and reflectivity give us information about the asteroids' density, internal structure, and surface properties. The images also show surface features such as impact craters, and irregularities, which can often be traced across the surface as the object rotates.

# Asteroids

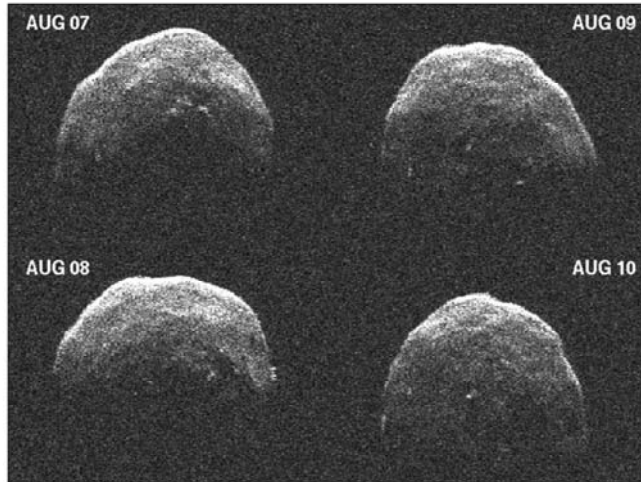
Arecibo delay-Doppler radar image of  
NEA 1999 KW4 (D ~ 1.5 km)



- Several binary asteroid systems have now been discovered by radar. These were determined to be binary systems from a combination of Goldstone and Arecibo radar observations. These close pairs of asteroids must be recently formed, perhaps by tidal forces on a previous close approach to the Earth. The lifetime of such a binary system against collisional disruption is quite short.

# Asteroids

Arecibo delay-Doppler radar image of  
NEA 1999 KW4 (D ~ 1.5 km)



UNIVERSITY OF AMSTERDAM

Radio Astronomy - 5214RAAS6Y

ASTRON

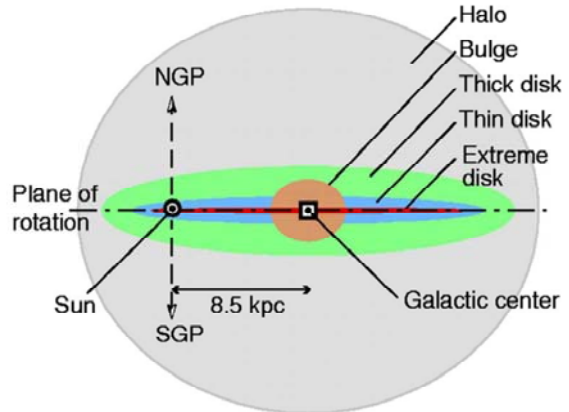
- A series of images can be used to derive a three-dimensional shape model. That shape can be highly irregular, and is a strong constraint on formation mechanisms. The shape of some very small objects is surprisingly spherical, which suggests a rubble pile with no internal strength.
- And in a worst-case (impact) scenario, the cost and use of any mitigation effort can be estimated by the object's size, shape, mass, spin state, and orbit, and by revealing if it is one body or a two-body system.

# Milky Way

- We observe: diffuse continuum emission from the disk
- 21 cm HI line emission from clouds
- Weak radio emission from all star types
- Radio emission from glowing HII clouds ionized by light from hot, young stars
- Some 300 radio supernova remnants
- Neutron stars observed as pulsars

# Milky Way

- Sketch shows main structures of MW
- Most objects to be discussed are in thin disk
- Associated with star formation...
- ...and star demise
- First, diffuse gas

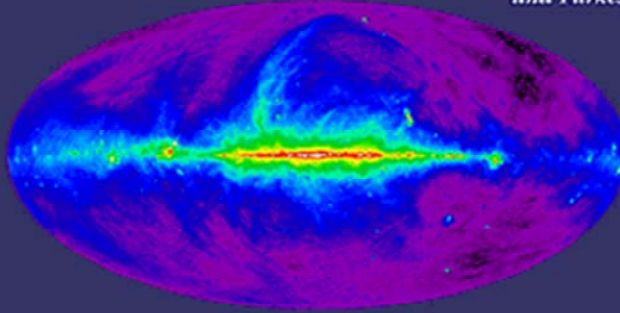


# Milky Way

In radio continuum, we see through the whole Milky Way

*Radio Continuum (408 MHz)*

*Bonn, Jodrell Bank,  
and Parkes*



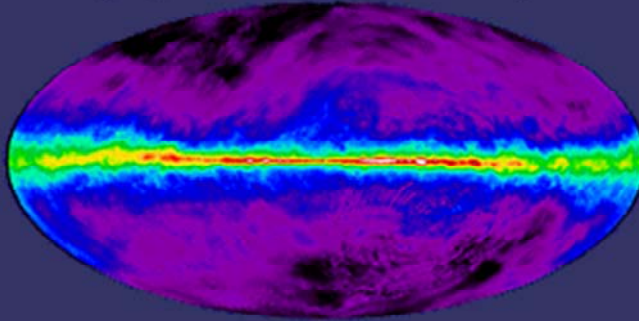
The North Polar Spur, sticking out of the North of the Galactic plane, is part of a nearby supernova remnant, or a local hot interstellar bubble created by winds of young, hot stars and several supernova explosions.

# Milky Way

Dust also has no influence on the 21 cm HI line

*Atomic Hydrogen*

*21 cm Dickey-Lockman*



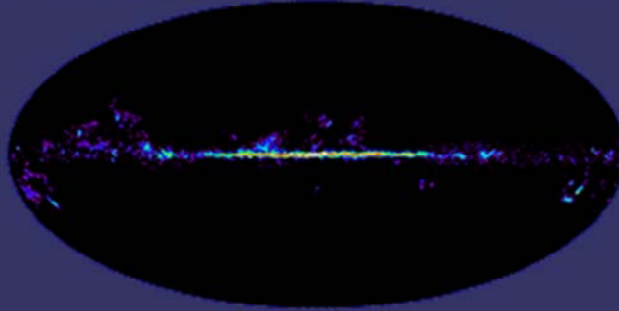
- A component of the radio emission from the Milky Way comes from the spin flip transition of the hydrogen atoms (Atomic Hydrogen, HI) in the interstellar medium.

# Milky Way

The CO line at 2.6 mm is a surrogate for H<sub>2</sub>

*Molecular Hydrogen*

*115 GHz Columbia-GISS*



- Molecular Hydrogen (H<sub>2</sub>) is hard to detect directly. The symmetric H<sub>2</sub> molecule has no permanent dipole moment and hence does not emit a detectable spectral line at radio frequencies. The CO line is generally used as a tracer.

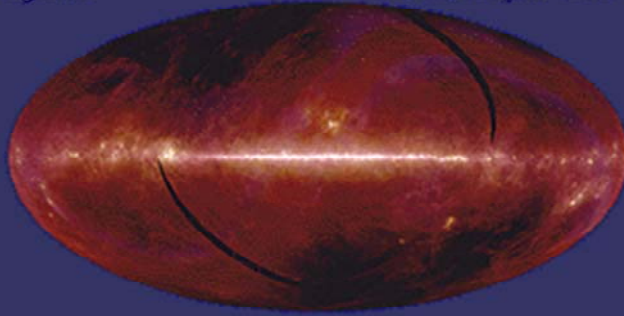


# Milky Way

Most IR emission is unblocked (and comes from hot dust)

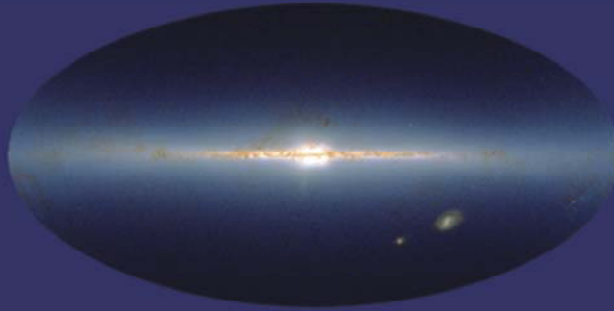
*Infrared*

*12, 60, 100  $\mu\text{m}$  IRAS*



# Milky Way

Near IR (2  $\mu\text{m}$ ) bulge unobstructed by dust



# Milky Way

In the galactic plane, little light gets through the dust

*Optical*

*A. Mellinger Photomosaic*

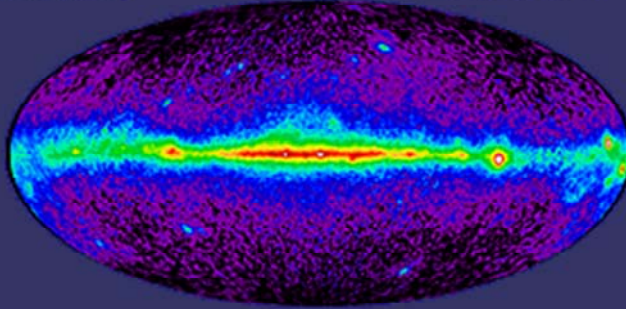


# Milky Way

High energy  $\gamma$ -rays, unobstructed and closely linked to gas

*Gamma Ray*

*>100MeV CGRO/EGRET*



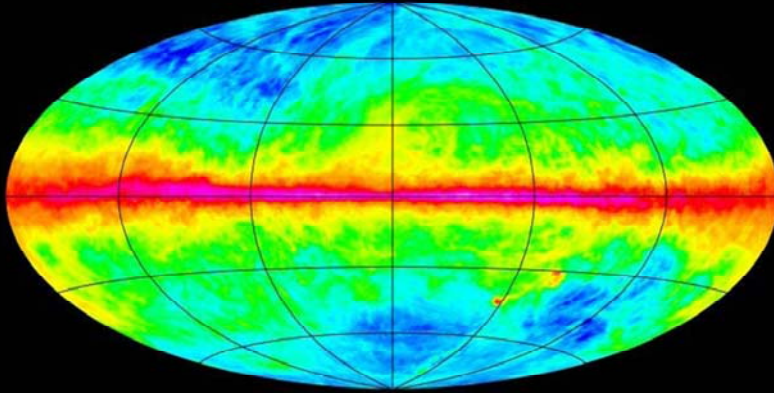
# Milky Way

These images show both diffuse and discrete sources:

- The 21 cm HI and 2.6 mm CO mainly come from diffuse clouds of H and H<sub>2</sub>
- Much of the 408 MHz radio continuum is from discrete sources (clouds of ionized gas, shocks from supernovae)
- X-ray emission from hot, shocked gas, and from binaries & various stars
- IR from hot dust and cool stars

# Milky Way

Milky Way is difficult to study as we are in it

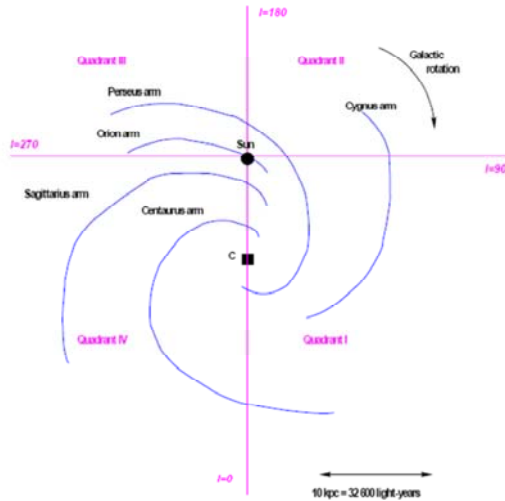


- This image is the Leiden/Argentine/Bonn (LAB) Survey of Galactic HI: Final data release of the combined LDS and IAR surveys with improved stray-radiation corrections

# Milky Way

4 quadrants: 4 quadrants:

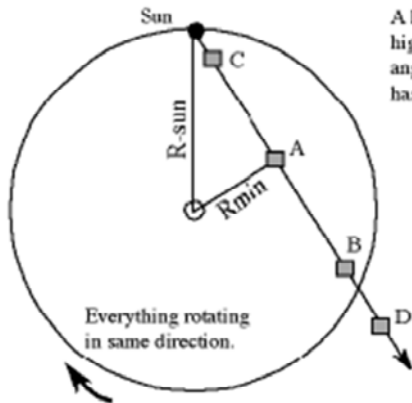
I & III, gas moves away; II & IV, gas approaches



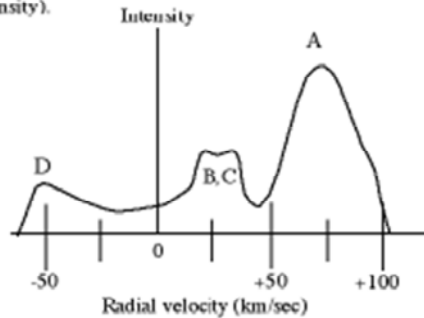
- Based on the apparent motions of the gas and stars, the Milky way is divided in 4 quadrants.

# Milky Way

To map motion in Milky Way we must assign peaks to locations



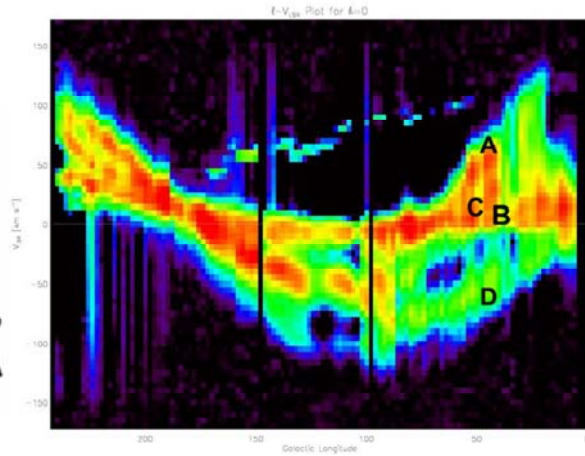
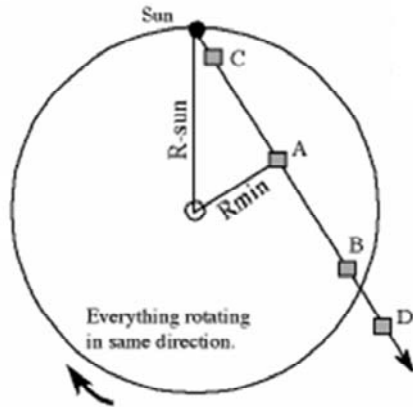
A has greatest angular speed and moving fastest away from sun. A has higher density of H. B & C moving at about same angular speed > sun's angular speed. D is outside solar distance—slower angular speed and has less material (density).





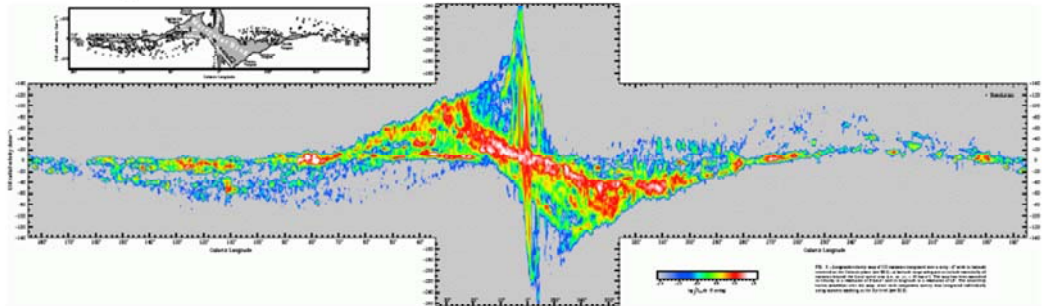
# Milky Way

The HI in the Milky Way disk, as position vs. velocity



# Milky Way

The line emission (especially HI and CO) gives speed of gas

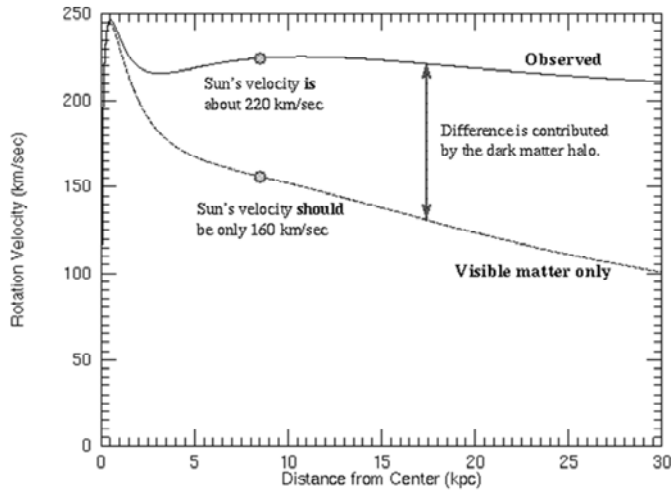


CO in the MW plane, motion relative to Sun  
Positive velocity = away from us

- This same curve here seen in high resolution. Note the 180 degree shift from the previous slide.
- Based on 115 GHz data, this shows the differential rotation in our MW
- Also note the sharp “Nuclear Disk” feature at the centre
- [https://openaccess.leidenuniv.nl/bitstream/handle/1887/6534/ApJ\\_322\\_706\\_720.pdf?sequence=1](https://openaccess.leidenuniv.nl/bitstream/handle/1887/6534/ApJ_322_706_720.pdf?sequence=1)

# Milky Way

Orbital speed in MW is almost constant outside of center



# Stellar Lifecycles

Large complexes of dust, H II regions, molecules:  
cradle of stars



- In astronomy, anything not “gas” is “dust”. Here is the star formatting region in Orion.

# Stellar Lifecycles

Proto-stars are usually shrouded in dust

Plus molecules like CO



- The contours in the image are the Horsehead in CO (taken with the BIMA mm array) overlaid on a VLT optical image. The CO contours show where the dense clumps of material are within the dark cloud.



# Stellar Lifecycles

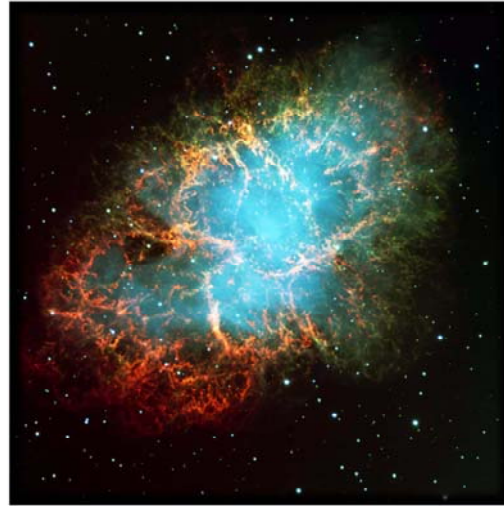
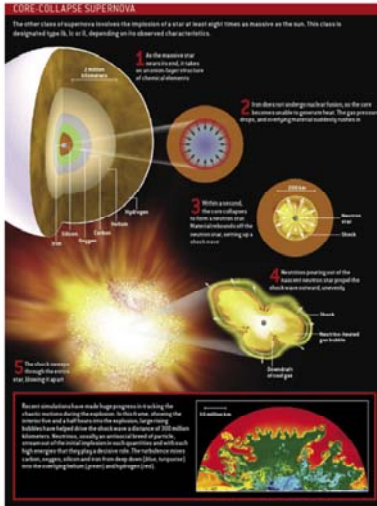
Millimeter band is particularly rich in molecular emission: ALMA now allows for *mm imaging*



- Where this was previously done for a single beam, or direction, ALMA now provides excellent /imaging/ in the mm range.

# Stellar Lifecycles

Massive stars then explode in supernovae

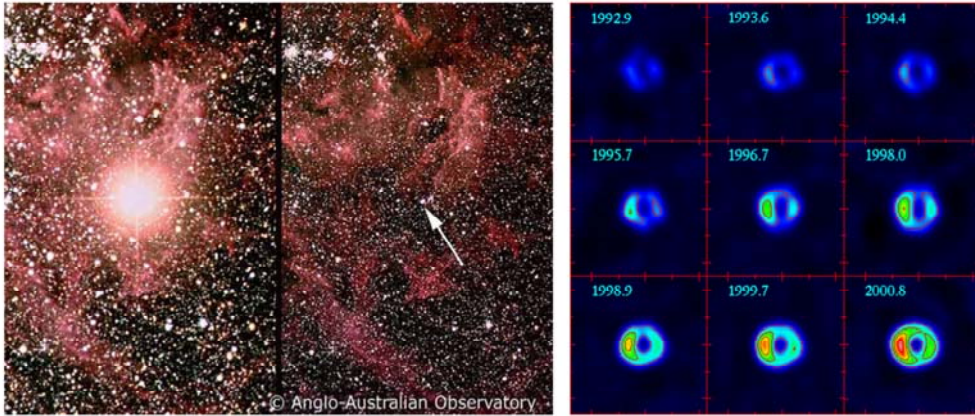


- I will next discuss supernovae, and the compact objects formed in these, neutron stars and black holes.



# Stellar Lifecycles

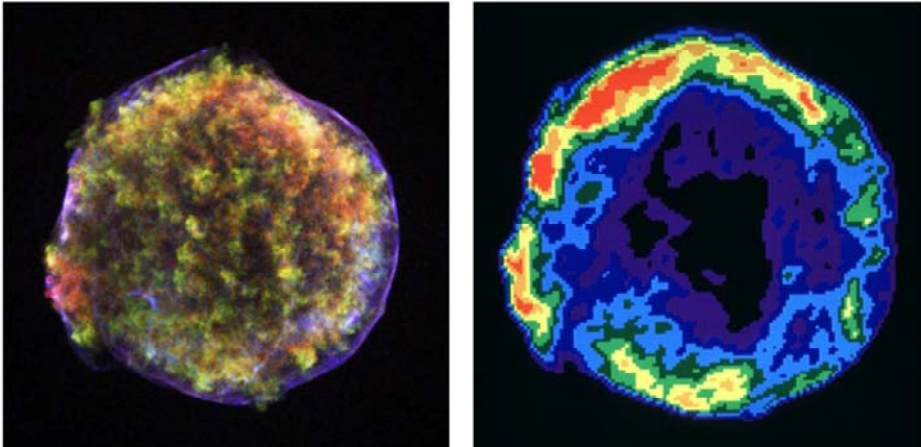
Explosion produces a shell-like shock (cf. SN87a):



- Supernova SN87a. On the right, 3-cm observations with ATCA, the Australia Telescope Compact Array.

# Stellar Lifecycles

Then a supernova remnant. The SNR from the “nova” seen by Tycho in 1572 (x-ray, radio)



- Left is a Chandra X-ray image of SN 1572. Red 0.95-1.26 keV, Green 1.63-2.26 keV. These are thermal radiation. Blue is 4.1-6.1 keV, and non-thermal, from the shocks. Note there is the outer shock, but also a reverse shock that moves back in (best seen in the bottom half).
- Image taken with the VLA. Note how only the shocked regions shine.

# Stellar Lifecycles

Supernova remnant of the SN 1006 AD

X-rays thermal,  $10^6\text{K}$  gas  
(red) heated in shock

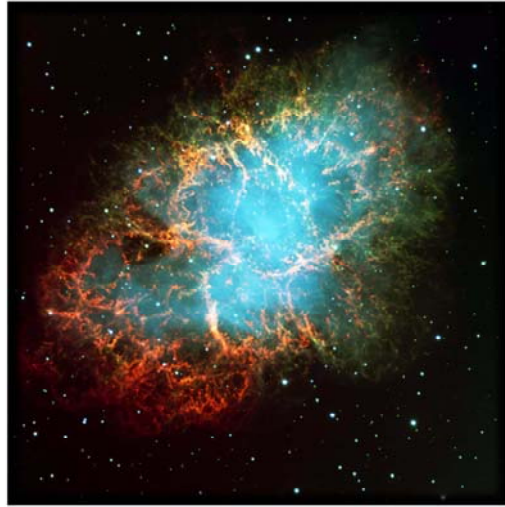
Shock boosts electrons to  
 $\sim c$  : synchrotron (blue)

Synchrotron causes radio  
(next lecture)



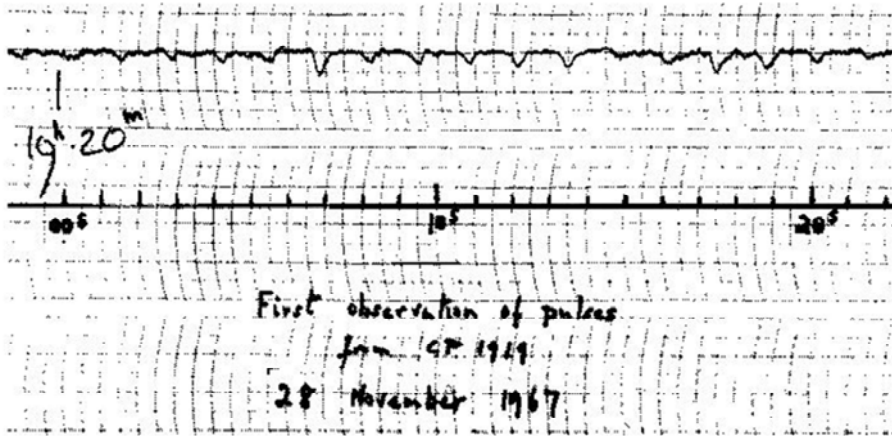
# Stellar Lifecycles

Some supernova remnants continue to be powered ..  
but by what?



# Pulsars

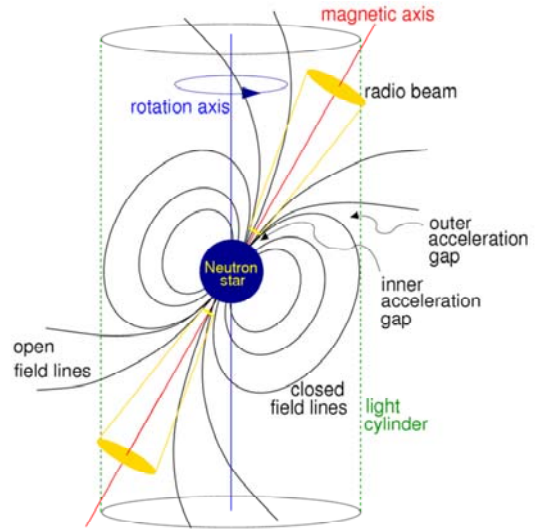
Discovered serendipitously in 1967 during a low-frequency survey of extragalactic radio sources that scintillate in the interplanetary plasma.



- Just as stars twinkle but planets don't, scintillation tells you what the angular size of a radio source is. Hewish and Bell conducted a survey for that with the Cambridge Array,

# Pulsars

## Radio emission generated near polar cap

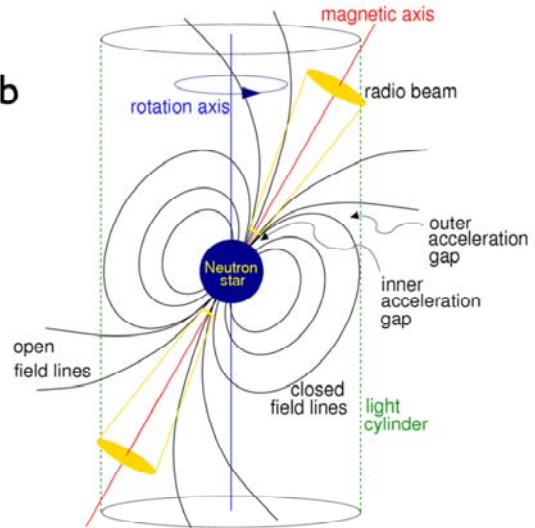


- Due to the pulsar rotation, plasma is continuously flung out of the magnetosphere. In the vacuums that are formed, particles can be accelerated to high enough energies to emit.
- “Inner” gap, right over the surface, makes radio.
- “Outer” gap makes most high-energy emission.

# Pulsars

Radio emission generated near polar cap

Most energy goes in  
“Poynting flux”. For Crab  
 $10^5$  Solar luminosities



- That radio emission is only a <1% fraction of the energy loss. Most energy goes out in the very low frequency radio wave that is caused by the spin of this magnet.
- For a 1-s pulsar, this means a 1Hz “radio” wave, called the “Poynting flux” This energy loss is what causes the observed pulsar spin down.

# Pulsars & the ISM

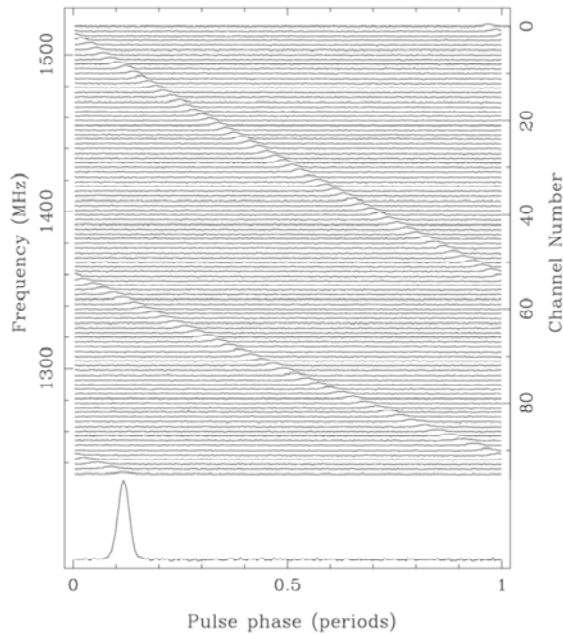
With their sharp and short-duration pulse profiles and very high brightness temperatures, pulsars are unique probes of the interstellar medium (ISM). Variable group speed introduces *dispersion delay*:

$$\nu_p = \left( \frac{e^2 n_e}{\pi m_e} \right)^{1/2} \approx 8.97 \text{ kHz} \times \left( \frac{n_e}{\text{cm}^{-3}} \right)^{1/2}$$

$$v_g \approx c \left( 1 - \frac{\nu_p^2}{2\nu^2} \right)$$



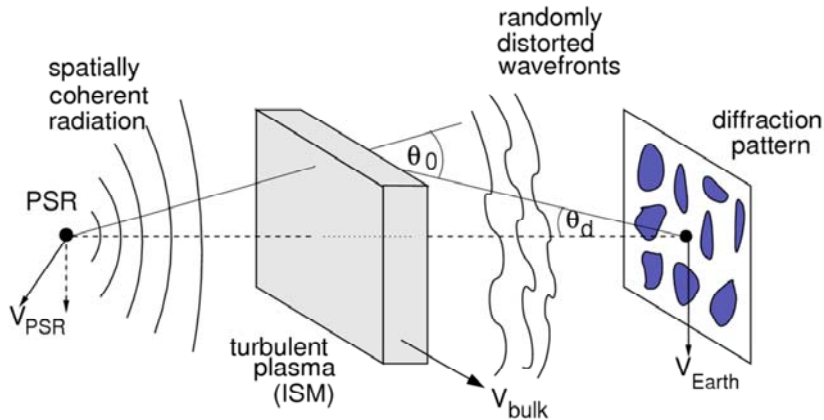
# Pulsars & the ISM



- This is pulsar data that is already folded on the pulsar period. Following the pulsar down from 1500 MHz, you can see the delay is already larger than the pulsar period at 1350 MHz!
- Pulse dispersion shown in this Parkes observation of the 128 ms pulsar B1356–60. The dispersion measure is  $295 \text{ cm}^{-3} \text{ pc}$ . The quadratic frequency dependence of the dispersion delay is clearly visible.

# Pulsars & the ISM

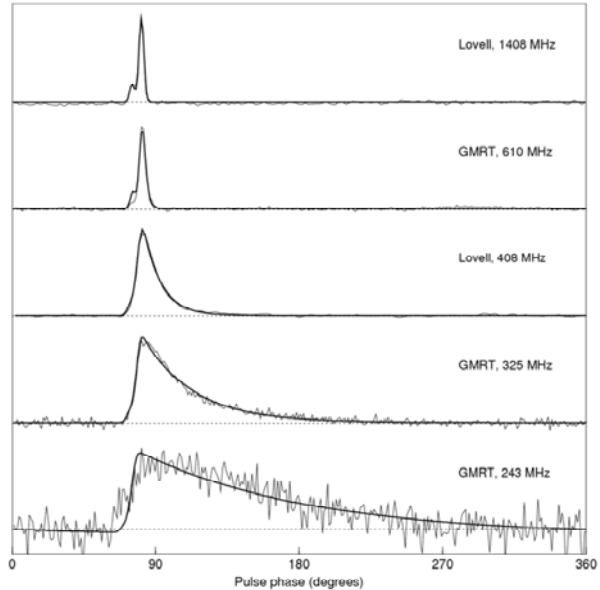
Inhomogeneities in the ISM cause small-angle deviations in the paths of the radio waves.



- This multi-path propagation causes emission that takes “the long way around” to arrive later than emission that goes straight.

# Pulsars & the ISM

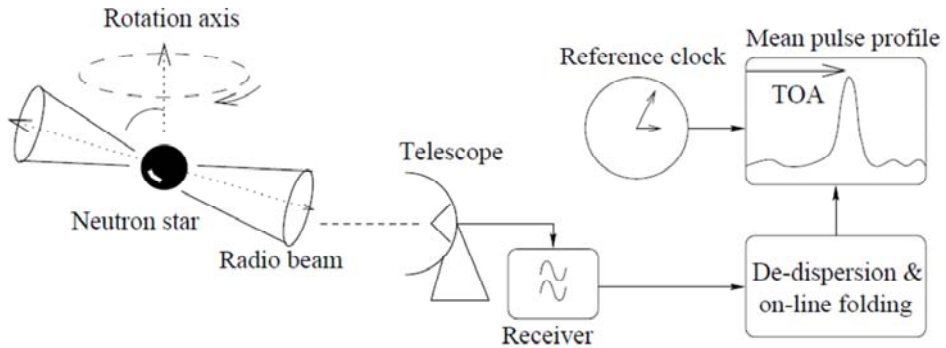
These cause  
scattering tails on  
pulse profiles



- For longer wavelengths, this effect increases strongly (as  $f^{-4}$ ) with frequency
- Pulse profiles for PSR B1831-03 observed at five different frequencies with the Lovell telescope and the GMRT. These data show clearly the increasing effects of scatter broadening at lower frequencies.

# Pulsar Timing

Clock-like stability of pulsars means that precise monitoring of pulsar rotations allows for study of rich variety of physics phenomena



- The basic concept of a pulsar timing observation.

# Pulsar Timing

The attainable precision is extreme:

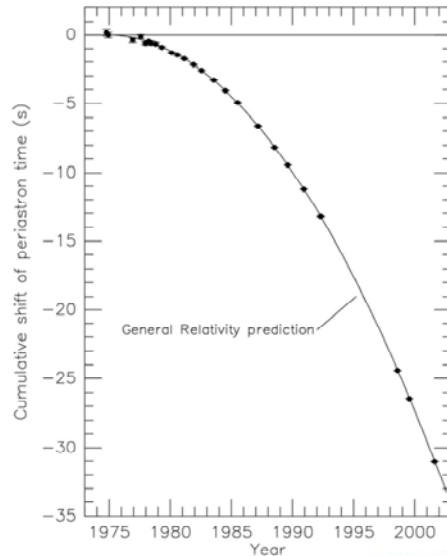
Table 1 PSR J0437–4715 physical parameters

Right ascension, $\alpha$ (J2000) ...	04 <sup>h</sup> 37 <sup>m</sup> 15 <sup>s</sup> .7865145(7)
Declination, $\delta$ (J2000) .....	-47°15'08".461584(8)
$\mu_\alpha$ (mas yr <sup>-1</sup> ) .....	121.438(6)
$\mu_\delta$ (mas yr <sup>-1</sup> ) .....	-71.438(7)
Annual parallax, $\pi$ (mas) .....	7.19(14)
Pulse period, $P$ (ms) .....	5.757451831072007(8)
Reference epoch (MJD) .....	51194.0
Period derivative, $\dot{P}$ (10 <sup>-20</sup> ) ..	5.72906(5)
Orbital period, $P_b$ (days) .....	5.741046(3)
$x$ (s) .....	3.36669157(14)
Orbital eccentricity, $e$ .....	0.000019186(5)
Epoch of periastron, $T_0$ (MJD) ..	51194.6239(8)
Longitude of periastron, $\omega$ (°) ..	1.20(5)
Longitude of ascension, $\Omega$ (°) ..	238(4)
Orbital inclination, $i$ (°) .....	42.75(9)
Companion mass, $m_2$ ( $M_\odot$ ) ...	0.236(17)
$\dot{P}_b$ (10 <sup>-12</sup> ) .....	3.64(20)
$\dot{\omega}$ (°yr <sup>-1</sup> ) .....	0.016(10)

- Millisecond pulsar timing example. A timing ephemeris for the nearby MSP J0437–4715 by van Straten et al. 2001. This is one of the best "timing" pulsars known (post-fit RMS timing residuals of 100 ns), and this measurement is one of the most accurate astrometric measurements ever made. In addition, the timing accuracy allowed a fundamentally new test of general relativity.

# Pulsar Timing

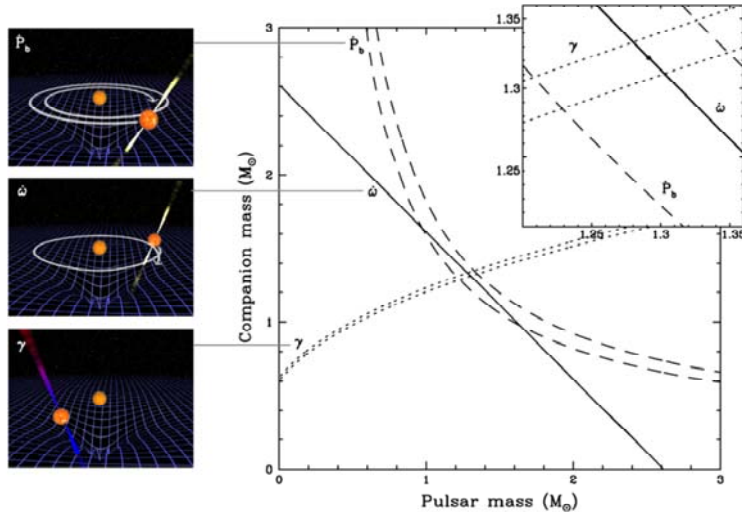
The attainable precision is extreme:



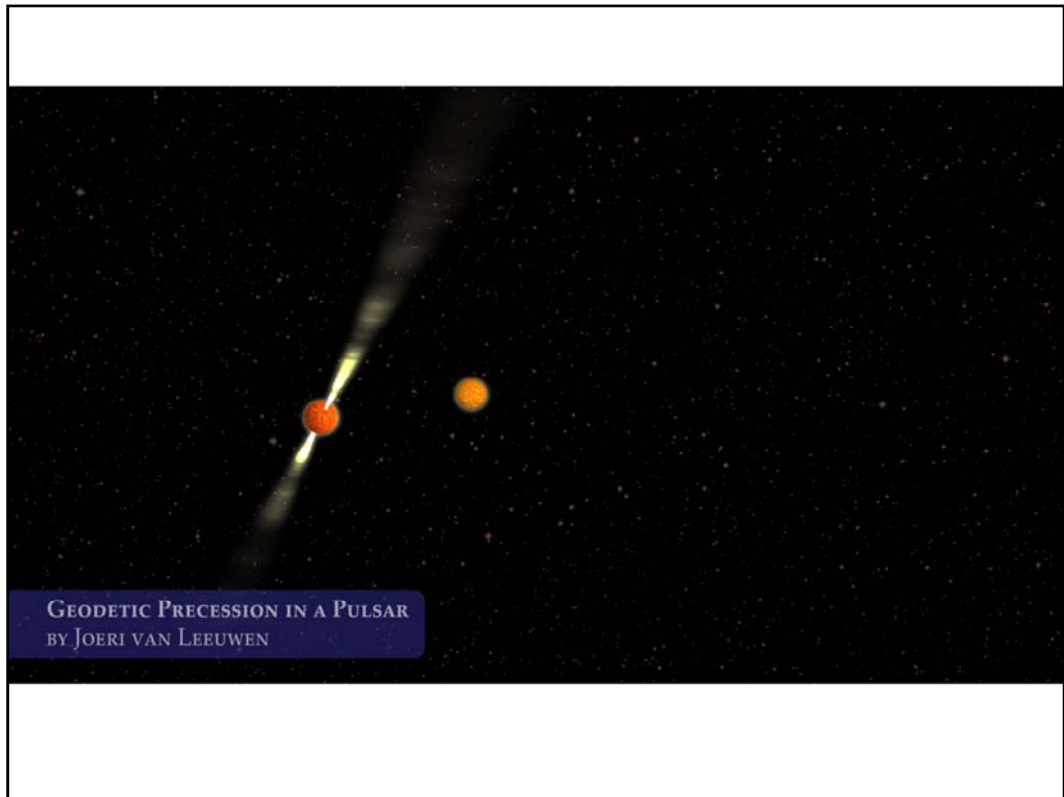
- Timing results for the Hulse-Taylor binary pulsar B1913+16. The left panel shows the mass vs. mass plot for the pulsar and its companion neutron star. The three lines correspond to the three measured post-Keplerian parameters. The right panel shows the periastron shift caused by the decay of the orbit via emission of gravitational radiation. The detection of gravitational radiation resulted in a Nobel prize for Hulse and Taylor.

# Pulsar Timing

Young pulsar J1906+0746, and the double pulsar, provide some of the best tests of general relativity.

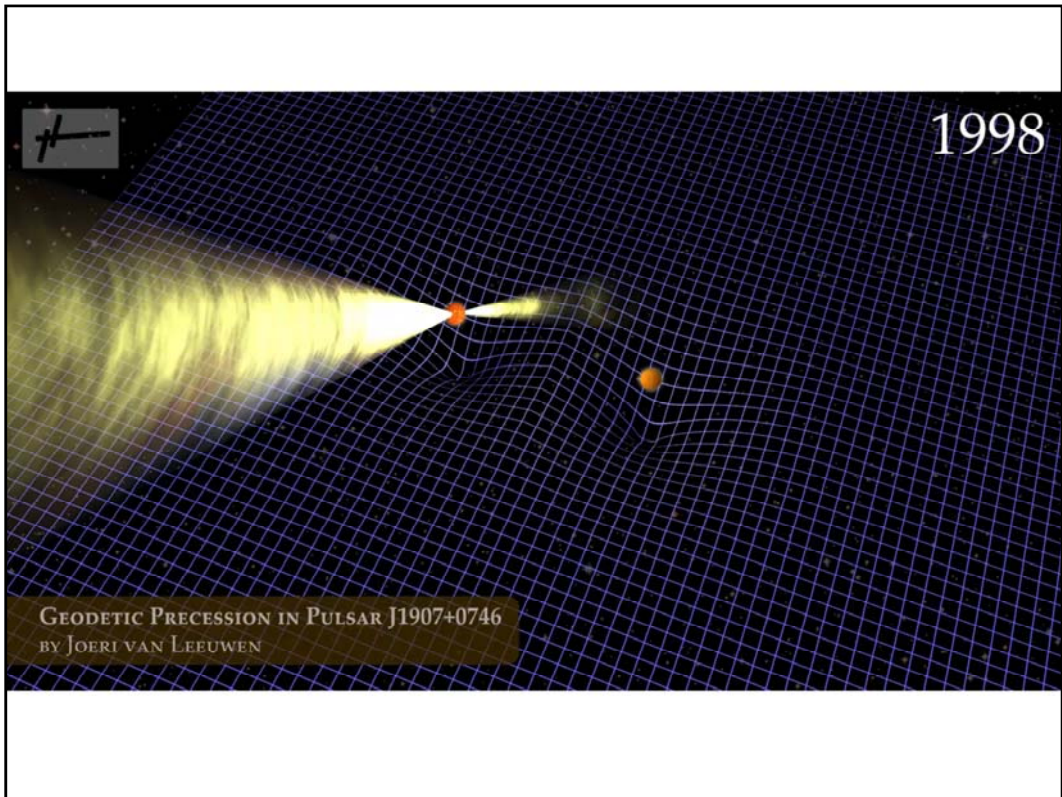


- PSR J0737–3039 mass vs. mass diagram. As in Figure 3, the diagram shows lines corresponding to the post-Keplerian parameters measured for the system. In this case, though, six parameters were measured, including the mass ratio  $R$  since both neutron stars are pulsar clocks. These measurements have tested GR to  $\sim 0.05\%$



- PSR J0737–3039 mass vs. mass diagram. As in Figure 3, the diagram shows lines corresponding to the post-Keplerian parameters measured for the system. In this case, though, six parameters were measured, including the mass ratio  $R$  since both neutron stars are pulsar clocks. These measurements have tested GR to  $\sim 0.05\%$

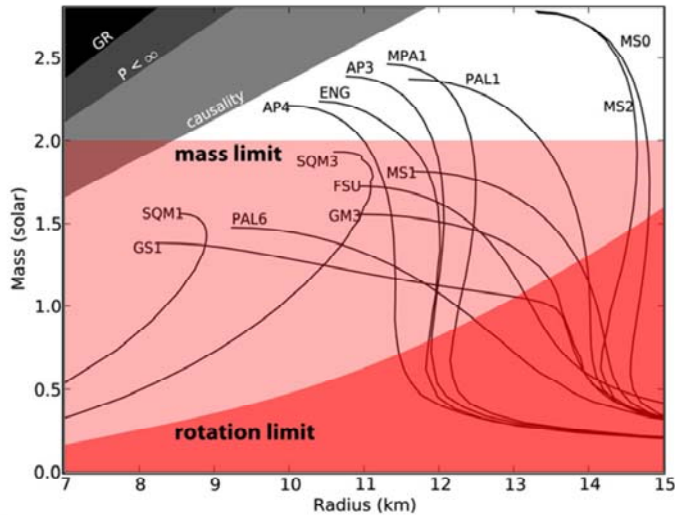




- PSR J0737–3039 mass vs. mass diagram. As in Figure 3, the diagram shows lines corresponding to the post-Keplerian parameters measured for the system. In this case, though, six parameters were measured, including the mass ratio  $R$  since both neutron stars are pulsar clocks. These measurements have tested GR to  $\sim 0.05\%$

# Pulsar Timing

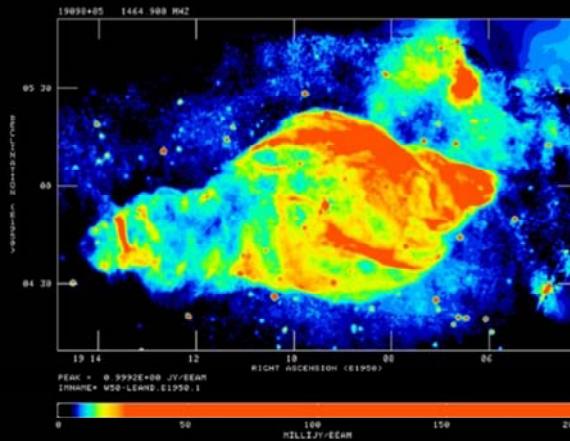
One of the few ways to “weigh” a star, and determine its composition:



- The Equation of State (EoS) of pulsar determines how the density changes with increasing pressure. It can be e.g. “stiff” (not compressible) or “soft” (compressible).
- Different EoSs have different maximum masses, at which the star collapses to a black hole.
- Finding a massive pulsar can thus rule out EoSs.
- The 2.0 solar Mass pulsar is the most constraining measurement so far, and it is one of Jason’s results!

# Black Holes

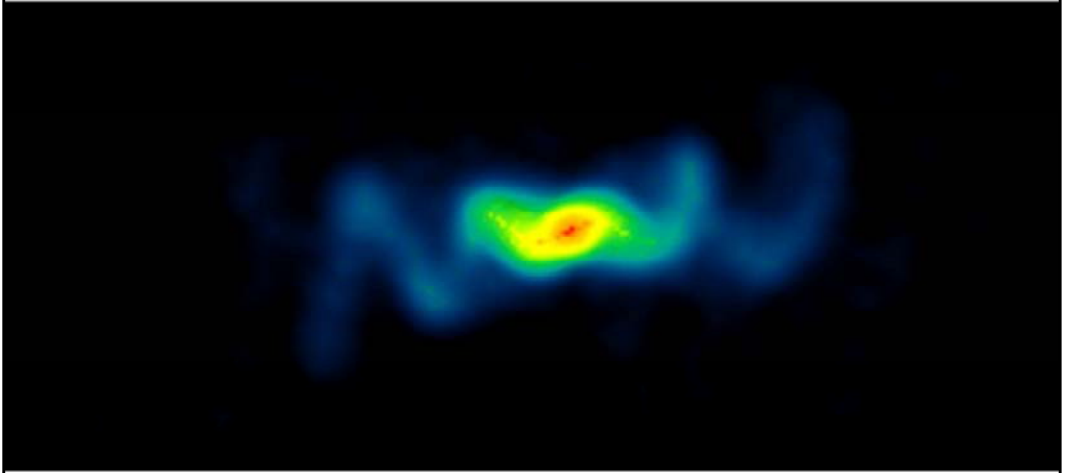
Supernova remnant W50 (~20 kyr) with the central microquasar SS433



- The other compact source possibly formed in a super nova remnant (here, see W50) is a black hole. If these interact with a companion star, and form radio jets, they are called “microquasar” (a somewhat strange name; a NS binary system forming jets is sometimes also called a microquasar).

# Black Holes

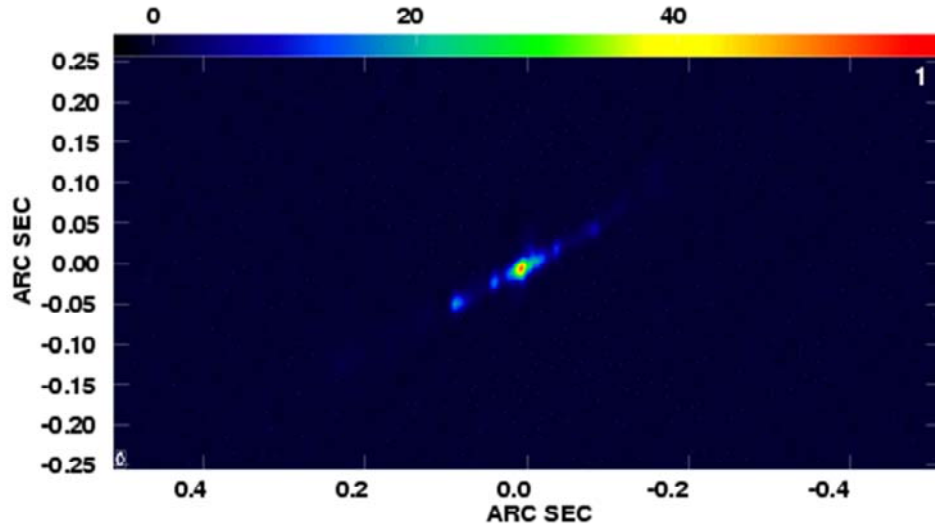
Eclipsing X-ray binary system, compact-object mass indicates black hole



- VLA image of the microquasar SS 433, in the constellation Aquila. This image was made using 10 hours of observing time on the VLA, which was configured to provide the greatest amount of detail in the image. The image shows the corkscrew-like path of subatomic particles that were shot from the core of the microquasar.

# Black Holes

Eclipsing X-ray binary system



UNIVERSITY OF AMSTERDAM

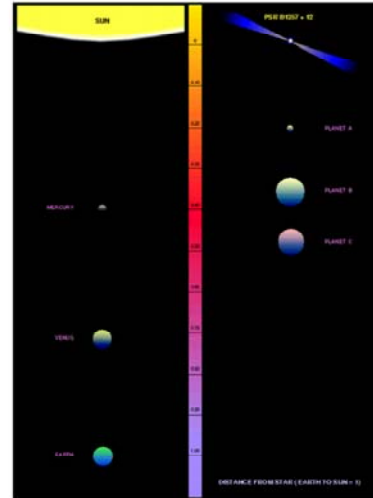
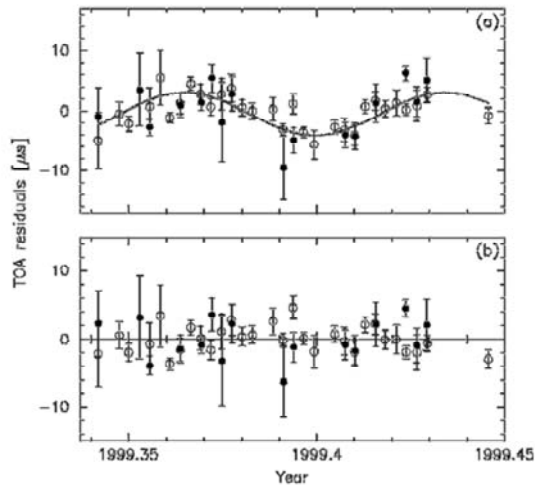
Radio Astronomy - 52I4RAAS6Y

ASTRON

- From this VLBA "Movie", the companion star is assumed to be  $11 M_{\text{sol}}$ , combined with a  $3 M_{\text{sol}}$  BH/NS

# Exoplanets

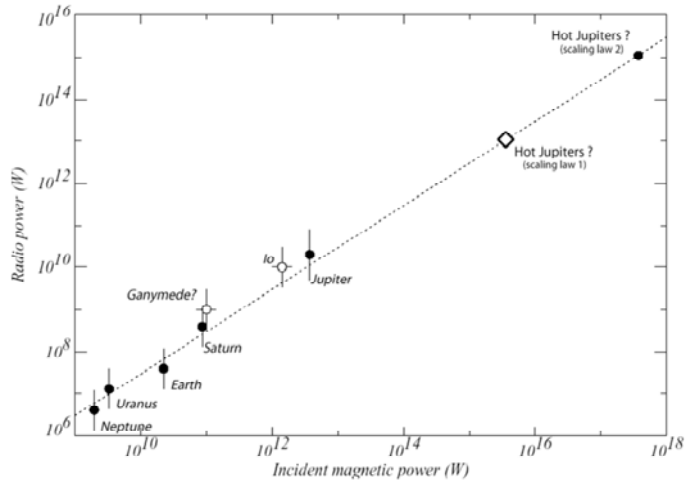
The first extra-solar planets were detected around a pulsar



- These were detected as timing anomalies in the pulsar signal.

# Exoplanets

Giant exoplanets around magnetic stars may be detectable with LOFAR

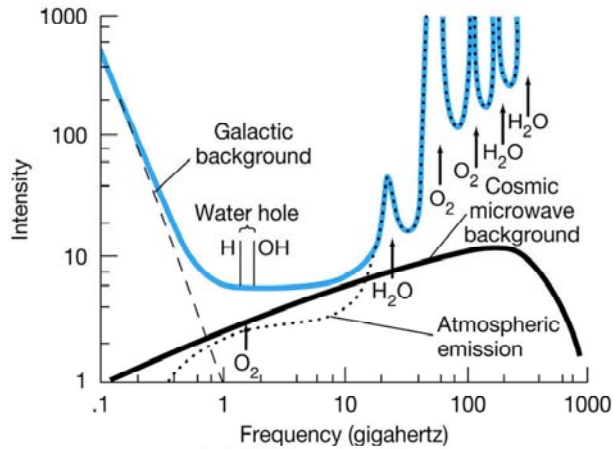


- Direct radio detection of exoplanets could be possible, if one extrapolates the Jupiter activity when orbiting a star with much higher magnetic power than the Sun.

# SETI

Intelligent life probably easiest to detect in radio

Naturally occurring radiation defines least “noisy” frequencies

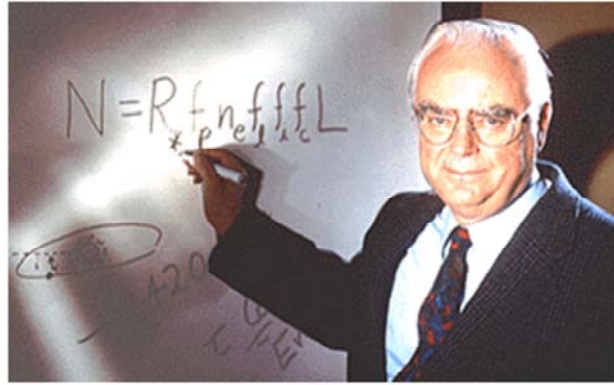


Copyright © 2005 Pearson Prentice Hall, Inc.



# SETI

This led Frank Drake to his equation for the number of planets we could communicate with



# SETI

Example:

Suppose there are  $\approx 10^{11}$  stars in Milky Way, but only 10% in “habitable zone”: leaves  $10^{10}$

Suppose 10% have planets: leaves  $10^9$

If 1% are like Earth, then  $10^7$  are left

Suppose 1% develop life: leaves  $10^5$

But if only 1% of life is intelligent: leaves  $10^3$

Suppose 10% develop communication: 100

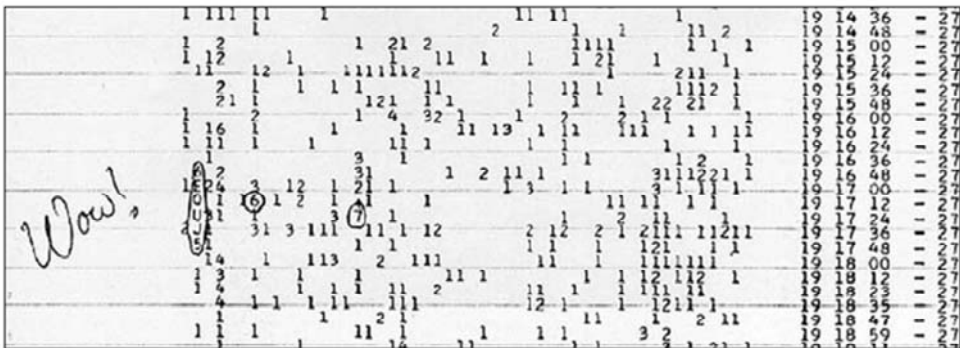
If communication lasts 1% of lifetime: 1 left

# SETI

Searches with Ohio, Arecibo, Nançay, LOFAR

Much overlap with pulsar searching

Some analysis done with SETI@home software



- The instrumentation used in SETI shows much overlap with that used for pulsar observing.
- LOFAR is doing a first pass of planets around two dozen nearby stars this year.

# SETI

Dedicated search telescope: *The Allen Telescope Array*



- When I was at Berkeley, Microsoft's Paul Allen wrote us a 50-million dollar check to build a telescope that would do radio astronomical imaging, pulsar searching (my responsibility) and SETI searching!
- Many new techniques were tried out for the first time, but no new pulsars were detected. And no SETI signals yet, either. Check <https://arxiv.org/abs/1607.04207>

# Questions?

- References and source material:
- <http://www.haystack.edu/edu/undergrad/materials/SSemission.pdf>
- <http://www.cv.nrao.edu/course/astr534/ERA.shtml>
- <http://link.springer.com/article/10.12942/lrsp-2006-2>
- [http://www.astron.nl/~leeuwen/course/RadioAstronomy\\_2017/Strom/](http://www.astron.nl/~leeuwen/course/RadioAstronomy_2017/Strom/)
- Kramer & Lorimer, Handbook of pulsar astronomy